Organic Rankine cycle as a waste heat recovery system for data centers: design and construction of a prototype

Sebastian Araya. Gerard F. Jones, Amy S. Fleischer Department of Mechanical Engineering Villanova University, Villanova, Pennsylvania, USA 19085

Abstract

As a result of constantly increasing data center utilization, many challenges have appeared for thermal engineers over the last few decades. Advanced cooling systems for servers are of significant interest, particularly, technologies which can also reduce electricity usage. One known technology called Organic Rankine Cycle (ORC) is considered a viable alternative for this purpose. It can both the heat from a server and then transfer the server heat into a power cycle to generate electricity.

This study consists of the design and construction of an experimental prototype of 20kW of waste heat, representing two common rack servers operating at full capacity. The range of server waste heat temperatures is between 60°C to 85°C, which is far below the normal operating range for ORCs. This ultra-low-grade waste heat leads to an expected thermal efficiency between 2%-8%. Tests on the experimental rig showed a maximum thermal efficiency of 3.33%. The system is both absorbing all the waste heat from the data center and at the same time providing an economic benefit back to the data center in form of electricity. Through experimental investigation, this study provides the first evidence for using ORC system as a valid solution for ultra-low-grade waste heat recovery.

Key words: Organic Rankine Cycle, data center, ultra-low-grade, waste heat recovery, cooling system.

Nomenclature

- Temperature (°C)
- P Absolute pressure (Psi, kPa)
- W Work rate or power (W)
- Q Heat transfer rate (W)
- I Rate of exergy destruction (W)
- m Mass flow rate (kg/s)
- h Specific enthalpy (kJ/kg)
- s Specific entropy (kJ/kg)
- C_p Specific heat capacity at constant pressure (kJ/kg K)
- η Efficiency
- τ Torque (Nm)
- u Uncertainty
- N Shaft rotational speed (RPM)
- V Voltage (V)
- A Current (A)

Subscripts

- 0 Reference state
- 1 ORC state 1
- 2 ORC state 2
- ORC state 3
 ORC state 4
- ref ORC refrigerant

- I First law
- If Second law
- s Isentropic
- pu ORC pump
- ev ORC evaporator
- ex ORC expander
- co ORC condenser
- con Condensing
- sat Saturation
- HW Hot water cycle
- CW Chilled water cycle
- Th Thermal
- Me Mechanical
- El Electrical
- c Carnot
- L Cold reservoir
- H Hot reservoir
- b Belt
- PS Power supply
- su Suction
- di Discharge

1. Introduction

Data centers have become an essential component in information technology (IT). In data centers, racks of hundreds or thousands of servers are responsible for the processing and storing of critical information. In order to provide fully operational and reliable servers, robust cooling infrastructures were integrated into the data centers to remove the heat generated from the servers [1]. On the other hand, cooling systems have become a major portion of the total data center energy consumption [2]. It evaluated that the typical energy consumed by the cooling infrastructures constituted about 40-50% of the total energy consumption in a data center [3][4]. Thus, extensive improvements in cooling systems have been a major challenge in thermal engineering [5]. While data center cooling systems typically absorb the heat dissipated from the servers and release it to the ambient, alternatives such as waste heat recovery systems have been proposed to reuse the heat dissipated from servers before realizing it to the ambient, so the total energy consumption in a data center will be reduced. Recovering the waste heat through technologies such as the Organic Rankine Cycle (ORC) and the Absorption Refrigeration (AR) were proposed and modeled by Ebrahimi et al [1], [6]. It was found that both technologies bring economic benefits and are suitable for data center operating conditions. AR systems provide extra cooling by reducing the cooling energy consumption of the facility, while the ORC system creates on-site electricity generation. The ORC is preferred due to that the system exhibits more flexibility in the use of the electricity generation. The simplicity of the system makes it reliable, and low maintenance cost is typically needed for the

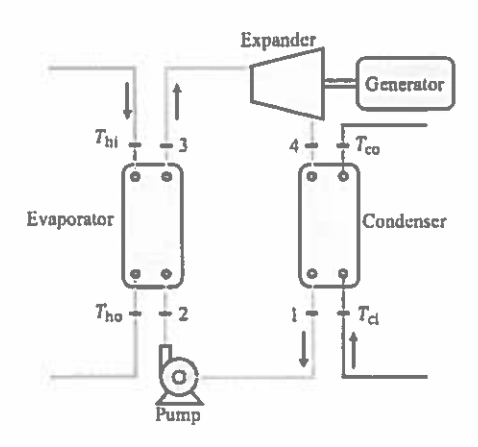


Figure 1: Schematic representation of an ORC

ORC components. On the other hand, AR main application is focused on assist the data center cooling systems by providing more cooling through the heat recovery. In addition, the AR system is a more complex system than the ORC system due to the use of chemical processing system included and maintenance cost can be more significant.

The interest for studying ORC as a power cycle technology has been running for many decades. An ORC is similar to a Steam Rankine Cycle (SRC) in its main components. However, an ORC is different from a SRC due to the quality, or grade of heat source required. The SRC quality heat source is higher than the

ORC heat quality source where the heat temperature operates over 370°C [7]. In contrast, ORCs typically operate in the range from 150°C to 350°C. Examples of ORC heat source applications are commonly in geothermal, biomass, solar, desalination systems and waste heat recovery [8]. The temperature range used in this study, 60°C – 85°C, is far below the normal operating range for ORC and is considered to be ultra-low-grade. The ultra-low-grade heat is usually not considered to be worth recovering, but recent review paper by Ebrahimi et al [1] has predicted it to be economically viable.

The ORC is a power cycle that uses heat to generate electrical power. The cycle uses a pump where fluid is pressurized and pumped to an evaporator. Then the evaporator receives heat through an external heat source to boil the ORC fluid. The vapor fluid goes to an expander, which is attached to a generator. Electrical power will be generated when the vapor expands though the expander. Next, the expanded vapor moves to the condenser where the fluid is condensed and carried back to the pump. Some specific types of ORC working fluid make the system suitable for low grade heat sources. Mostly used organic compounds include Hydrofluorocarbons (HFCs), for that they perform appropriate thermal properties at low saturation temperatures for low grade heat applications [9], [10].

The work presented in this paper takes the concept of ORC for data center operations beyond the modeling stage to small prototype. A lab scale prototype has been designed, scaled to the typical waste heat conditions of two server racks at full workload reflecting the amount of 20kW. A hot water cycle

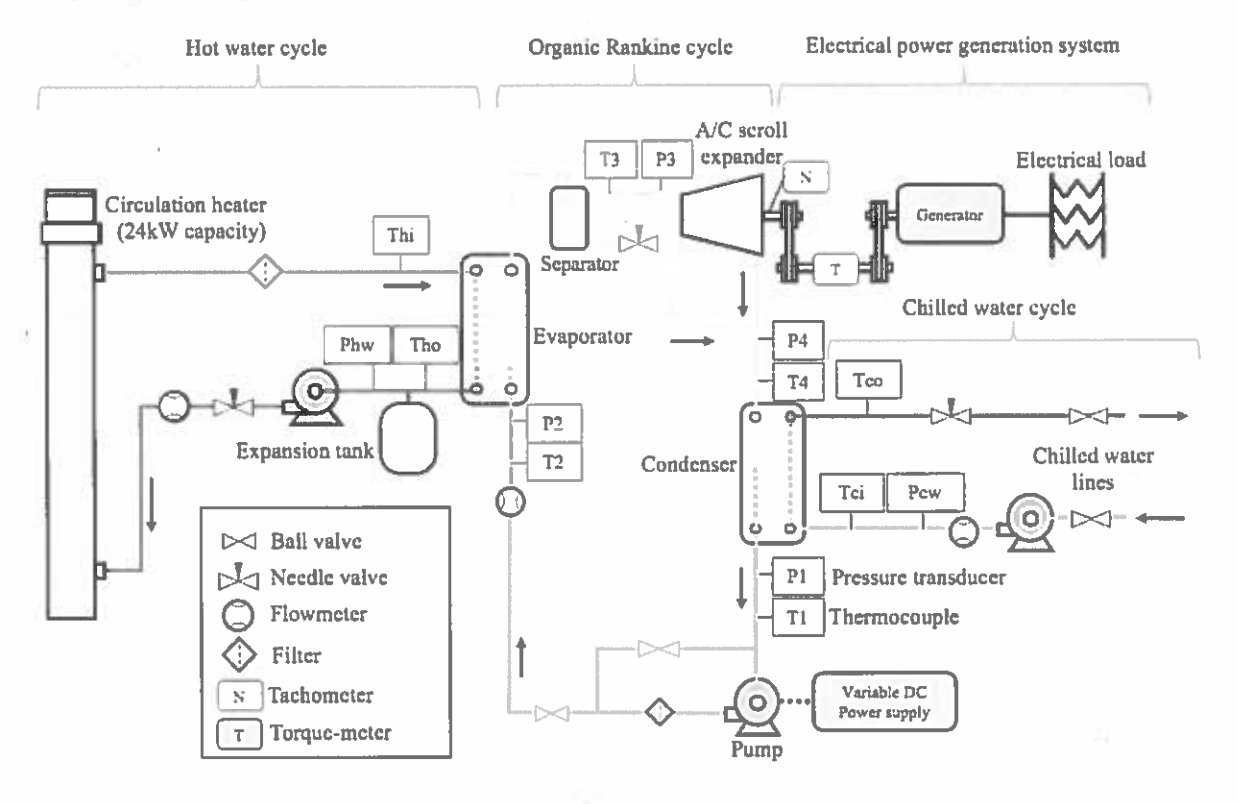


Figure 2: Schematic representation of the experimental ORC prototype

Table 1
Definition of ORC thermal parameters by using energy balances

Thermal parameter	Equation	
Power supplied to the pump [W]	$\dot{W}_{\mathrm{pu}} = \dot{m}_{\mathrm{ref}}(h_2 - h_1)$	(1)
Refrigerant heat transfer in the evaporator [W]	$\dot{Q}_{\rm ev}=\dot{m}_{\rm ref}(h_3-h_2)$	(2)
Power produced by the expander [W]	$\dot{W}_{\rm ex} = \dot{m}_{\rm ref}(h_4 - h_3)$	(3)
Refrigerant heat transfer in the condenser [W]	$\dot{Q}_{\rm co}=\dot{m}_{\rm ref}(h_1-h_4)$	(4)
Pump isentropic efficiency [-]	$\eta_{\mathrm{pu}} = \frac{h_{21} - h_1}{h_2 - h_2}$	(5)
Expander isentropic efficiency [-]	$\eta_{ex} = \frac{h_4 - h_3}{h_{4s} - h_1}$	(6)
ORC thermal efficiency [-]	$\eta_1 = \frac{\dot{W}_{\rm ex} - \dot{W}_{\rm pu}}{\dot{Q}_{\rm ex}}$	(7)
Hot water heat transfer [W]	$\dot{Q}_{\rm HW} = \dot{m}_{\rm HW} C_{\rm p,HW} (T_{\rm hi} - T_{\rm ho})$	(8)
Cold water heat transfer [W]	$\dot{Q}_{\mathrm{CW}} = \dot{m}_{\mathrm{CW}} C_{\mathrm{p,CW}} (T_{\mathrm{cl}} - T_{\mathrm{eq}})$	(9)

Table 2
Definition of ORC thermal parameters by using entropy balances

Thermal parameter	Equation	
Pump exergy destruction (W)	$I_{\rm pu}=m_{\rm ref}T_0(s_2-s_1)$	(10)
Evaporator exergy destruction [W]	$I_{\text{ev}} = m_{\text{ref}} T_0 \left[(s_3 - s_2) - \frac{(h_3 - h_2)}{T_{\text{H}}} \right]$	(11)
ORC expander exergy destruction [W]	$\dot{I}_{\rm ex} = \dot{m}_{\rm ref} T_{\rm 0} (s_4 - s_3)$	(12)
Condenser exergy destruction [W]	$I_{\mathrm{co}} = \dot{m}_{\mathrm{ref}} T_0 \left[(s_1 - s_4) - \frac{(h_1 - h_4)}{T_{\mathrm{L}}} \right]$	(13)
Carnot cfficiency [-]	$\eta_c = 1 - \frac{T_L}{T_H}$	(14)
Second law efficiency [-]	$\eta_{11} = \frac{\eta_1}{n}$	(15)

was used to represent the heat dissipated from server racks. Experimental tests were run on this system at various waste heat temperatures and mass flow rates to provide a thorough understanding of ORC performance. Therefore, this study can facilitate future improvements of data center waste heat recovery systems. More details of the experimental design are demonstrated in our previous work [11]. A MATLAB thermodynamic model was developed to estimate the size of the main components of the ORC prototype. In addition, the modeling was used to validate thermal performance of the system under different waste heat conditions. In this ORC prototype, the expander power output increases more than 50% with additional 20°C of waste heat temperature and absorbs additional 40% of waste heat. Therefore, findings in this study proves the viability of ORC application for data center operations at ultra-low-grade waste heat conditions.

2. The ORC thermodynamic modeling

Prior to the construction of the lab scale ORC prototype, an analysis of the ORC thermodynamic performance was carried



Figure 3: Experimental ORC test rig

out through a MATLAB thermodynamic modelling. The modelling requires the thermodynamic states of the ORC shown in Fig. 1. With the corresponding temperatures and pressures, thermal properties such as specific enthalpies, entropies and specific heats were obtained through the NIST REFPROP database 8.0 [12]. The modelling allows to obtain the expected thermal efficiency, power output and suitable component size required for the ORC prototype, as shown in the previous work [11]. For the analysis of the experiment, the ORC thermal parameters were calculated based on the energy balances and entropy balances of the main ORC components. To obtain the ORC thermal parameters, the following assumptions were made: steady-state condition, constant thermal properties and negligible pressure drop through the piping and heat exchangers.

The energy balance leads to the expression for the heat transfer in the evaporator, heat transfer in the condenser, power supplied by the pump, power generated by the expander. In addition, the isentropic efficiencies of the pump and expander and the thermal efficiency were calculated based on the equations shown in Table 1. The entropy balance leads to the expression for the exergy destruction for each main ORC component, Carnot efficiency and second law efficiency. The exergy destruction calculations will help address where improvements should be made to improve the experiment's performance.

3. The ORC experiment setup

In the experiment, the ORC heat source is a hot water cycle as shown in Fig. 2 (right side). The hot water cycle is able to provide up to 20kW of heat with pressurized water of over 100°C temperatures. The pressured water is pumped by a hot water circulation pump, with its mass flow rate is controlled and set by a needle valve, and measured by a paddle flowmeter. The heat is generated by a Watlow circulation heater with 24kW of maximum capacity. The water temperature is set by a temperature controller. To avoid thermal expansion issues, an expansion tank is attached to the cycle.

A photo of the experimental ORC is shown in Fig. 3. The system uses refrigerant R245fa as the ORC working fluid. The working fluid selection is based on previous studies that proved the best working fluid for ORCs applied in data center environments was R245fa [1]. The refrigerant R245fa exhibits better thermal properties for the system, including low boiling temperatures, low pressures and low environmental impact. A rotary vane pump is used as the ORC pump. The pump is selected due to the ORC working fluid requirement for evaporation, which needs high saturation pressure at low flow rate. Therefore, this positive displacement type of pump with such features is selected. A Coriolis flowmeter is used to measure the refrigerant mass flow rate. A brazed plate heat exchanger is used as the evaporator, which transfers heat between the hot water source and the refrigerant. The condenser is the same a brazed plate heat exchanger as the evaporator. The condenser is located at the top of the experimental rig to provide enough static pressure and NPSH for the pump. In addition, pipe insulation was used to reduce the heat lost through the pipe system, including all components in the experiment.

A separator is located after the evaporator to ensure that only vapor goes to the expander, while the retained liquid in the separator bypasses to the condenser. The expander used for this experiment is an open-drive automotive A/C scroll compressor. For the choice of the expander, a positive displacement machine is favorable for this small size ORC system, which requires low expander inlet temperature, low flow rate, low rotational speed and high pressure ratio [13]. The selection of an A/C scroll compressor is based on its wide output power range, minimal maintenance cost and availability. The scroll compressor is used in reverse as an expander machine by removing its internal check valve in the compressor discharge compartment [14]. The expander shaft is connected to a rotary torque meter through pulleys and belts. A tachometer reads the rotational speed of the expander shaft. A single-phase AC generator is connected to the expander shaft to provide electrical power to a load.

The chilled water supply from the building is used to condense the refrigerant by removing heat in the ORC condenser, as it is shown in Fig. 2 (left side). By using a booster pump, a needle valve and a paddle flowmeter, the mass flow rate of the chilled water can be controlled, set and measured accordingly.

4. Experimental measurements

The test conditions focused on evaluating the impact of waste heat recovery temperature on the system thermal performance. This evaluated conditions quantify the expected performance for different data center conditions. The evaluated conditions include six waste heat temperatures from 60°C to 85°C in increments of 5°C. The ORC mass flow rate is a variable. Therefore, the amount of waste heat is considered a variable.

The systematic uncertainty of the measurement was calculated to identify the error from instrumentation. The measuring device uncertainties from manufacturer's data sheets are shown in Table 3. The thermal parameter uncertainties were calculated

Table 3
Measured parameter uncertainties

Measured parameter	Instrument of measurement	Uncertainty	
Temperature	mperature Thermocouple K-type 304 SS sheath, OMEGA		
Pressure	Pressure transducer PX309-200GV, OMEGA	±0.25% F.S.	
Refrigerant mass flow rate	Coriolis flowmeter, Micro Motion F025 series	±0.20% of rate	
Hot and chilled water flowrates	Paddle flowmeter, FTB4605, OMEGA	±1.50% of rate	
Expander shaft torque	Rotary torque meter, Lebow 1104-100	±0.10% of rate	
Expander shaft rotational speed	Inductive proximity sensor, Telemecanique sensor XS512B1PAL2	±4.00% of rate	

by using the Root Sum Squared (RSS) method [15], as shown in equation 16:

$$u_Y = \left[\sum_i \left(\frac{\partial Y}{\partial X_i} u_{X_i}\right)^2\right]^{1/2} \tag{16}$$

The thermal parameter uncertainties for 20kW of waste heat at 60°C and at 85°C are shown in Table 4.

5. Results and discussions

The results are organized as follows: heat transfer balances, supplied pump power and generated expander power, the system thermal efficiency, and exergy destruction of the main components of the system. In addition, the experimental results obtained in this study are validated with thermodynamic modeling.

Table 4
Measured parameter uncertainties for 20kW of waste heat

Thermal parameter	Uncertainty WHT 60°C	Uncertainty WHT 85°C	Relative error WHT 60°C	Relative error WHT 85°C
\dot{W}_{pu}	± 5.1 W	± 4.8 W	21.8 %	9.3 %
Q _{ev}	± 46.4 W	± 51.5 W	0.2 %	0.3 %
Wex	± 28.0 W	± 36.3 W	2.7 %	2.3 %
\dot{Q}_{co}	±41.1 W	± 40.6 W	0.2 %	0.2 %
η_{pu}	± 27.8 %	±11.8%	34.8 %	14.8 %
$\eta_{\rm ex}$	± 2.3 %	± 1.9 %	3.9 %	3.1 %
η_1	± 0.1 %	± 0.2 %	2.8 %	2.4 %
\dot{Q}_{HW}	± 614.2 W	± 668.3 W	3.07 %	3.34 %
Qcw	± 328.4 W	± 312.0 W	1.70 %	1.69 %
$I_{\rm pu}$	± 5.4 W	± 5.1 W	109.1 %	45.6 %
lev	± 72.5 W	± 71.3 W	7.7 %	5.7 %
iex	± 49.7 W	± 48.3 W	7.6 %	5.0 %
i,	± 88.2 W	± 85.2 W	7.3 %	6.9 %
η_c	± 0.2 %	± 0.2 %	1.4 %	1.5 %
η_{11}	± 1.0 %	± 0.9 %	3.1 %	2.7 %

5.1. Heat transfer through the cycles

The heat transfer through the evaporator and condenser are shown in Fig. 4. For each waste temperature from 60°C to 85°C, it is seen that the total heat transferred to the ORC ranged from 5.73kW at 60°C to 8.32kW at 85°C. There is a clear benefit of operating at higher temperatures as there will be greater heat recovery. In the evaporator, heat transfer of the hot water cycle and the refrigerant showed a good agreement in measurements, with a maximum discrepancy less than 10%. The ORC received heat from 5.42kW to 7.60kW at from 60°C to 85°C of waste heat temperature, respectively. The lower amount received than transferred results from the heat losses of the heat exchanger. In the condenser, heat transfer of the chilled water cycle and the refrigerant showed a better agreement than in the evaporator, with a discrepancy less than 3%. Since the discrepancy of heat transfer is smaller, the performance of the condenser seems to be more desirable than the evaporator. The ORC rejected heat was from 5.14kW to 7.16kW at from 60°C to 85°C of waste heat temperature, respectively. The lower amount of heat transferred to the chilled water is also expected due to heat losses. The lower performance of the evaporator may be explained in two reasons: first, the flowmeter used in the hot water cycle may have slight calibration errors, producing uncertainties in the calculations of heat delivered in the evaporator; second, possible fouling due to the accumulation of unwanted material into the evaporator.

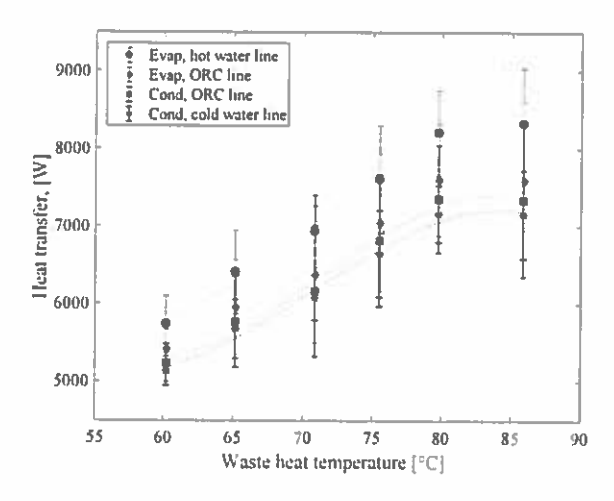


Figure 4: Energy balance of the evaporator and condenser

5.2. Pump supplied power and expander generated power

The power measurements obtained from the experiment are show in Fig. 5. The pump power was calculated by two ways to confirm agreement: the supplied thermal power (Th) obtained from eq. (1) and the supplied electrical power (El) from eq. (17):

$$\dot{W}_{pu_{el}} = V_{PS} A_{PS} \tag{17}$$

Where V_{PS} and A_{PS} are the voltage and current provided by the variable DC power supply, respectively. The minimum supplied thermal power was 24.72W at 60°C of waste heat

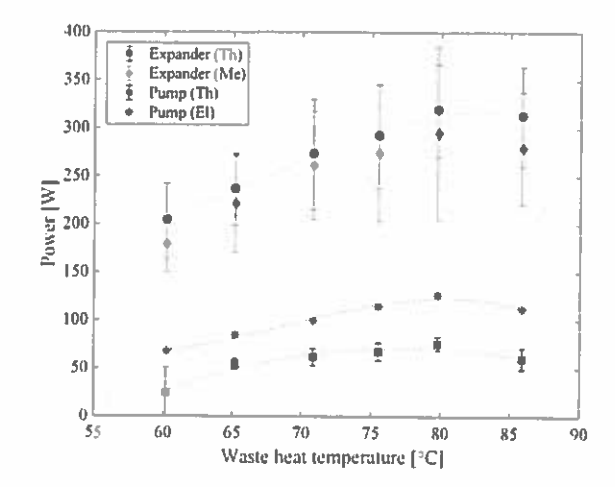


Figure 5: Pump power supplied, electrical (El) and thermal (Th) and Expander power generated, mechanical (Me) and thermal (Th)

temperature, and the maximum was 75.16W at 85°C (Fig. 4). The minimum supplied electrical power was 67.2W at 60°C of waste heat temperature, and the maximum was 126W at 85°C (Fig. 5). The conversion from electrical to thermal power in the pump showed the maximum relative difference of 63.2%. The low conversion was caused by heat loss in the DC motor from the electrical energy supplied. Therefore, the pump required higher electrical power to generate the pressure and flow rate of the working fluid demanded by the system, indicating that the pump isentropic efficiency was reduced and the ORC thermal efficiency was negatively affected.

The expander power was also calculated by two means: the generated thermal power (Th) obtained from eq. (3) and the generated mechanical power (Me) from eq. (18):

$$W_{cx_{me}} = \tau \frac{2\pi N}{60} \eta_b \tag{17}$$

Where τ is the torque generated by the expander shaft and measured by the torque-meter. N is the expander shaft rotational speed measured by the tachometer. And η_b is the efficiency of the belt, which connects the expander and torque-meter, with a fixed nominal value of 0.93.

As shown in Fig. 5, the generated thermal power achieved was 203.3W at 60°C and 318.9W at 80°C of waste heat temperature, representing an increment of power generation as high as of 56.9% with an additional 20°C of waste heat temperature and an increment of 40% of waste heat. This reveals that an ORC working with ultra-low-grade heat still recovers significant energy, thus making it an attractive solution for industrial scale data centers. The expander performance showed good agreement between the thermal and mechanical power when the waste heat temperature changed from 60°C to 85°C, with a maximum difference of 11.94%. The difference of thermal and mechanical power is due to the heat loss by friction from a belt-and-pulley, which connects the expander and torque-meter. However, the good agreement of

the results demonstrated validates the thermal power generated by the expander.

5.3. ORC performance and exergy destruction of the main components

The thermal performance of the cycle and exergy destruction of the main components are calculated and shown in Fig. 6. The thermal efficiency of the ORC varied from 3.19% to 3.33% over the waste heat temperature range. The thermal efficiency results are explained in section 5.4 according to the close relation with the expander performance.

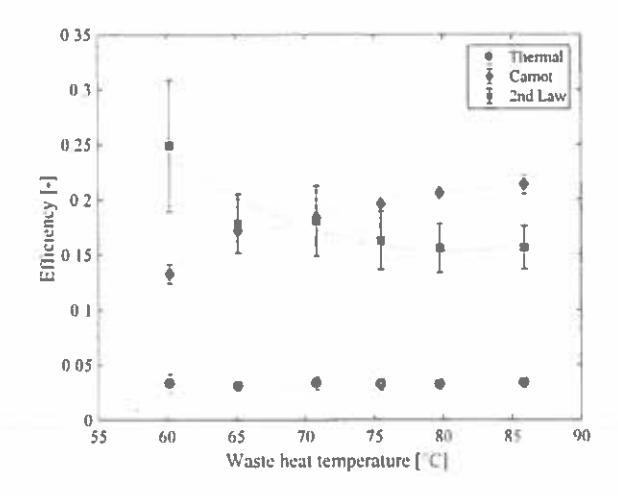


Figure 6: Thermal efficiency (circle), Carnot efficiency (diamond) and Second law efficiency (square)

The Carnot efficiency defined in eq. (14) increased from 13.24% to 21.35% when the waste heat temperature changed from 60°C to 85°C. It is because that according to its definition, the Carnot efficiency positively correlates to the hot reservoir T_H (waste heat temperature), and since the cold reservoir T_L (chilled water temperature) remains constant, higher T_H determines higher Carnot efficiency.

The second law efficiency, which is the ratio between the thermal efficiency and Carnot efficiency shown in eq. (15), decreased from 24.9% to 15.6%. Due to the fact that the thermal efficiency almost remained constant, the second law efficiency decreases when Carnot efficiency increases, indicating that ORC performance decreases at higher waste heat temperatures.

Figure 7 shows the results of exergy destruction of the main ORC components along the waste heat temperature range. The pump exergy destruction was from 21.44W to 71.61W when the waste heat temperature changed from 60°C to 85°C. The expander exergy destruction was from 162.48W to 281.08W at 60°C to 70°C, and consecutively decreased slightly to 226.47W to 85°C. The evaporator exergy destruction was from 157.69W to 557.28W when the waste heat temperature changed from 60°C to 85°C. The condenser exergy destruction was from 209.61W to 594.82W when the waste heat temperature changed from 60°C to 85°C.

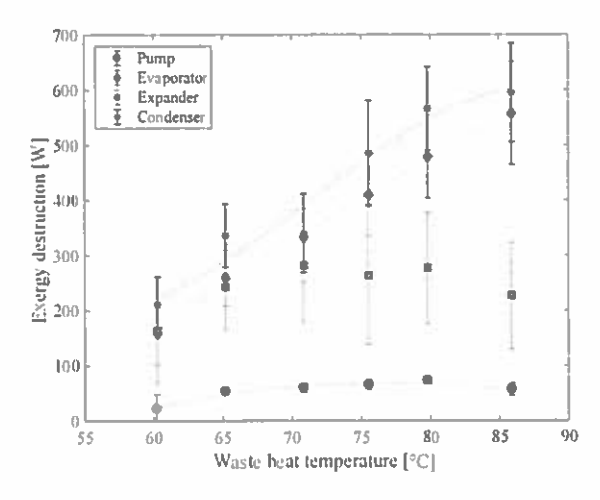


Figure 7: Exergy destruction of the main ORC components Pump (circle), Evaporator (diamond), Expander (square) and Condenser (star)

The pump provided the lowest exergy destruction compared with the other main ORC components, because the thermal power consumed for the pump is small compared with the other ORC components, and the exergy destruction is positively correlated to the thermal power consumed. Therefore, the pump provided the lowest exergy destruction in the tests. The exergy destruction in the heat exchangers showed a progressive increment as the waste heat temperature increased. The evaporator exergy destruction is due to the temperature difference between the hot water temperature and the refrigerant boiling saturation temperature increased over the waste heat temperatures. Therefore, in terms of exergy destruction, the heat transfer becomes more irreversible in the evaporator. The condenser exergy destruction increased due to the temperature difference between the chilled water temperature and the refrigerant condensing saturation temperature, where the heat transfer between the two fluids become more irreversible.

The inadequate refrigerant boiling saturation temperature and the refrigerant condensing saturation temperature can also be related to the expander performance since the saturation temperatures are directly related to the saturation pressures. This means that the pressure drop across the expander did not increase enough to optimize the exergy through the heat exchangers. Further analysis is presented in the next section.

5.4. The expander performance

The expander is known to be the key component of the ORC due to its functionality of generating power output. In this work, an A/C scroll compressor was used as expander in the ORC prototype. As seen in Fig. 8, the expander performance varied from 55.34% to 47.76% from 60°C to 85°C of waste heat temperature. The expander exergy destruction is shown in Fig. 8, where it shows negative correlation with the expander isentropic efficiency. The exergy destruction represents the work lost in the expansion process, and it causes the isentropic efficiency to decrease. In addition, the performance of the expander depends on the pressure ratio $(P_{\rm r})$, which relates to

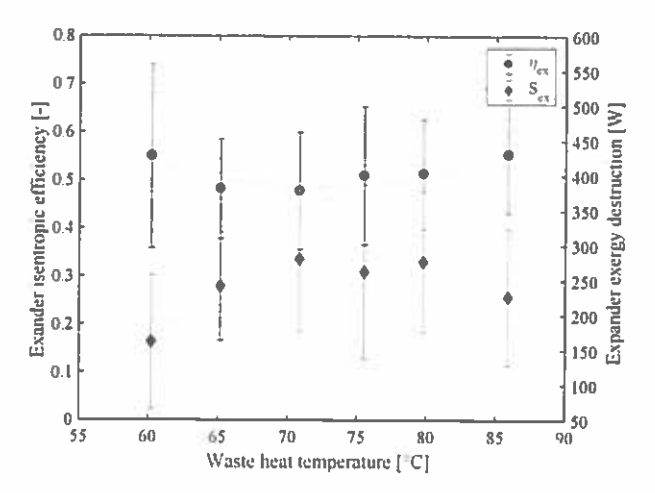


Figure 8: Expander isentropic efficiency (circle) and expander exergy destruction (diamond)

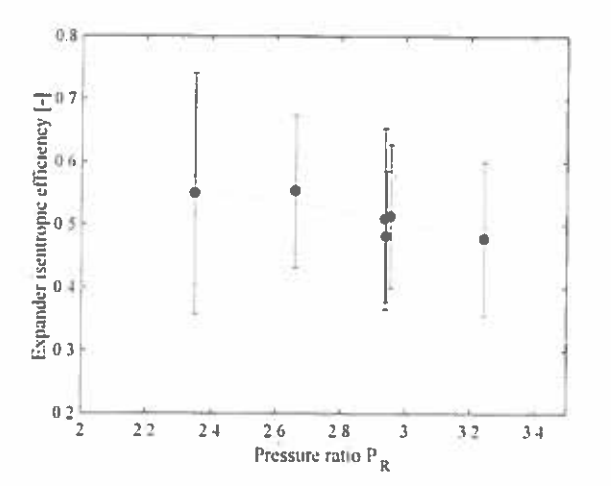


Figure 9: Relation between the expander isentropic efficiency vs the system pressure ratio

the suction expander pressure and discharge expander pressure as shown in eq. (18):

$$P_r = \frac{P_{su}}{P_{su}} \tag{18}$$

Volumetric expanders such as the A/C scroll compressor achieve the best performance when the system pressure ratio matches built-in internal pressure ratio of the expander. Figure 9 shows that the experimental result of the expander isentropic efficiency is dependent on the pressure ratio, where at higher P_r the efficiency becomes lower, which the expectation for this was the opposite. The reason for the decreasing expander efficiency shows an under-expansion process in the expander, meaning the internal pressure ratio of the expander is lower than the system pressure ratio. Therefore, the pressure at the end of the expansion process is higher than the pressure in the discharge line [13]. The pressure drop between the end of the expansion process and the expander discharge line is

represented as exergy destruction affecting negatively the expander efficiency.

Figure 10 shows that at higher outlet cold water temperature $T_{\rm co}$ the refrigerant condensing saturation temperature $T_{\rm sat_{con}}$ increases, and the pressure ratio $P_{\rm r}$ decreases. Therefore, the expander efficiency is directly related to the temperature $T_{\rm co}$ by connecting the pressure ratio effects.

The performance of the expander directly influences the thermal efficiency of the ORC system. Because the expander shows an under-expansion process within the working waste heat temperature range, an A/C scroll compressor of larger size may be preferred to achieve the optimal expander internal pressure ratio and the ORC system pressure ratio, and then the thermal efficiency of the system will be improved.

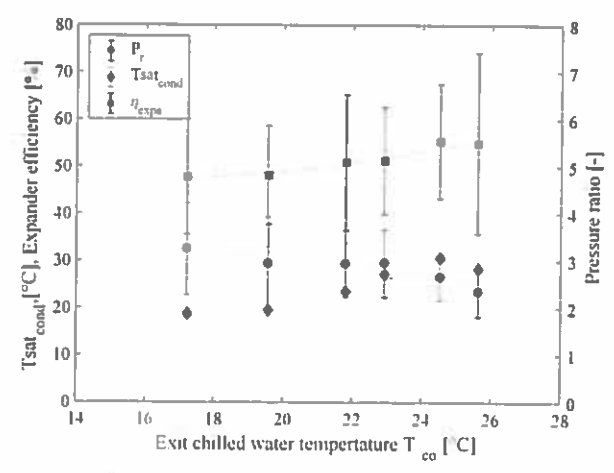
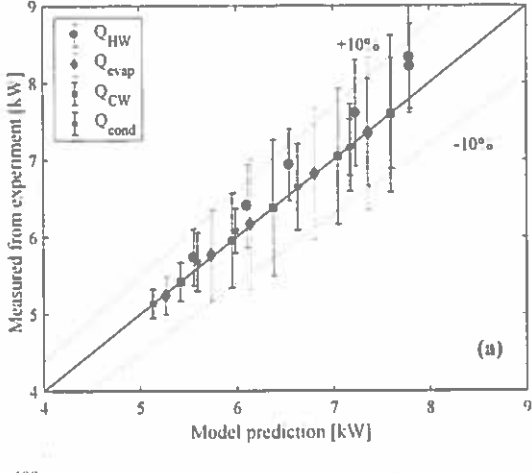


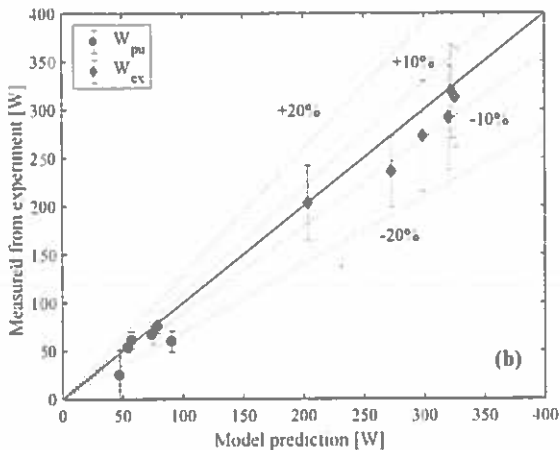
Figure 10: Relation among the system pressure ratio, expander isentropic efficiency and refrigerant condensing temperature v/s exit chilled water temperature

5.5. Validation of experimental measurements with thermodynamic modeling

The results of the ORC experimental set-up were compared with the thermodynamic modeling to validate the data obtained. The model utilized parameters measured in experiments such as temperatures, pressures and mass flow rates to find out the ORC parameters listed in Table 1-2.

In Figure 11a, the energy balance of the evaporator and condenser exhibited a good agreement with the thermodynamic model with an error of about 10%. In Figure 11b, the power supplied by the pump exhibited a fair agreement with the thermodynamic model with an error of about 20%. On the other hand, the expander power generated exhibited a better agreement with the thermodynamic model than the pump power, in which the error was about 10%. The overall thermal efficiency, as shown in Fig. 11c, exhibited a good agreement with the thermodynamic model with an error of 15%. Higher uncertainties mostly came from the instability of the pump measurements which affected the system thermal parameters. In the experiment, the suction side (state 1 Fig. 1) of the pump showed an unusual pressure fluctuations during the tests, thus causing more uncertainties to the measurements. Therefore, for





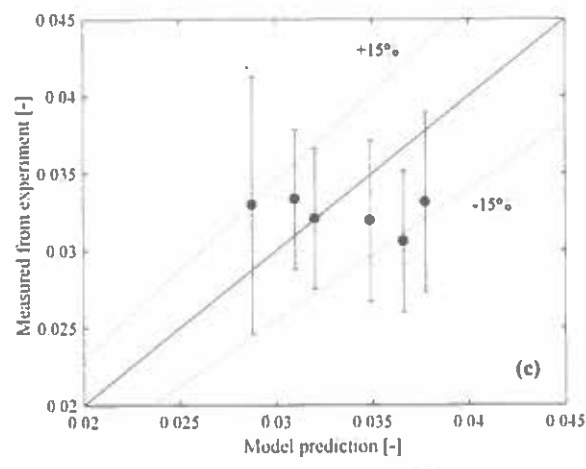


Figure 11: Experimental measurements v/s thermodynamic modeling results. (a) Energy balance, (b) Power supplied and generated, (c) ORC thermal efficiency

future tests, solutions to improve the pressure readings in the system are taking into account.

The results of the thermodynamic model successfully supported the data obtained from the experiment. The modeling will be viable to complement new scaling-up studies of ORCs in industrial applications such as data center environments.

6. Conclusions

An experimental study of an Organic Rankine Cycle (ORC) system using hot water cycle to represent waste heat from data center rack servers as heat source of 20kW was carried out. The evaluation of the thermal performance of the system with the operating conditions has been investigated. The lab scale ORC prototype achieved a maximum efficiency of 3.33%

A thermodynamic modeling to validate the experimental results by thermal parameters based by energy balance and entropy balance has been developed. The model predicts the heat transfer, power output and thermal efficiency.

The operating conditions for the ORC prototype were defined when the waste heat temperature was varied from 60°C to 85°C. Experimental results showed the expander power output increased 56.9% with an increment of waste heat temperature from 60°C to 80°C and an addition of 40% of waste heat. The increment reveals that the ORC still recovered significant energy at ultra-low-grade temperatures.

This study proves that the ORC technology is a valid solution for the waste heat ranges for data center environments, in which the waste heat is considered as ultra-low-grade heat. The ORC thermal efficiency is low but as the system is both absorbing all the waste heat from the data center and thus replacing the entire cooling apparatus and at the same time providing an economic benefit back to the data center in form of electricity. The low thermal efficiency does not preclude its viability. However, in the future means to reduce exergy destruction and improve thermal efficiency must be evaluated.

7. Acknowledgements

This work is supported by NSF IUCRC Award No. IIP-1738782. Any opinions, findings, and conclusions or recommendations expressed in this material are those of the author(s) and do not necessarily reflect the views of the National Science Foundation.

8. References

- [1] K. Ebrahimi, G. Jones, and A. Fleischer, A review of data center cooling technology, operating conditions and the corresponding low-grade waste heat recovery opportunities, vol. 31, 2014.
- [2] A. Shehabi et al., "United States Data Center Energy Usage Report," 2016. .
- [3] A. Capozzoli, M. Chinnici, M. Perino, and G. Serale, Review on Performance Metrics for Energy Efficiency in Data Center: The Role of Thermal Management, vol. 8945, 2015.
- [4] M. Dayarathna, Y. Wen, and R. Fan, "Data Center Energy Consumption Modeling: A Survey," IEEE Commun. Surv. Tutor., vol. 18, no. 1, pp. 732–794, Firstquarter 2016.
- [5] A. Capozzoli and G. Primiceri, "Cooling Systems in Data Centers: State of Art and Emerging Technologies," Energy Procedia, vol. 83, no. Supplement C, pp. 484–493, Dec. 2015.

- [6] K. Ebrahimi, G. F. Jones, and A. S. Fleischer, "The viability of ultra low temperature waste heat recovery using organic Rankine cycle in dual loop data center applications," Appl. Therm. Eng., vol. 126, no. Supplement C, pp. 393–406, Nov. 2017.
- [7] T. C. Hung, T. Y. Shai, and S. K. Wang, "A review of organic rankine cycles (ORCs) for the recovery of lowgrade waste heat," Energy, vol. 22, no. 7, pp. 661–667, Jul. 1997.
- [8] J. B. Obi, "State of Art on ORC Applications for Waste Heat Recovery and Micro-cogeneration for Installations up to 100kWe," Energy Procedia, vol. 82, no. Supplement C, pp. 994–1001, Dec. 2015.
- [9] H. Chen, D. Y. Goswami, and E. K. Stefanakos, "A review of thermodynamic cycles and working fluids for the conversion of low-grade heat," Renew. Sustain. Energy Rev., vol. 14, no. 9, pp. 3059–3067, Dec. 2010.
- [10] S. Quoilin, S. Declaye, A. Legros, L. Guillaume, and V. Lemort, "Working fluid selection and operating maps for Organic Rankine Cycle expansion machines," 2012.
- [11] S. Araya, G. F. Jones, and A. S. Fleischer, "The design and construction of a bench-top Organic Rankine Cycle for data center applications," in 2016 15th IEEE Intersociety Conference on Thermal and Thermomechanical Phenomena in Electronic Systems (ITherm), 2016, pp. 404-408.
- [12] E. W. Lemmon, M. L. Huber, and M. O. McLinden, "REFPROP, NIST Standard Reference Database 23, Version 8.0," Natl. Inst. Stand. Technol. Gaithersburg MD, 2007.
- [13] V. Lemort, S. Declaye, and S. Quoilin, "Experimental characterization of a hermetic scroll expander for use in a micro-scale Rankine cycle," Proc. Inst. Mech. Eng. Part J. Power Energy, vol. 226, no. 1, pp. 126–136, 2012.
- [14] P. Song, M. Wei, L. Shi, S. N. Danish, and C. Ma, "A review of scroll expanders for organic Rankine cycle systems," Appl. Therm. Eng., vol. 75, no. Supplement C, pp. 54–64, Jan. 2015.
- [15] R. B. Abernethy, R. P. Benedict, and R. B. Dowdell, "ASME Measurement Uncertainty," J. Fluids Eng., vol. 107, no. 2, pp. 161–164. Jun. 1985.

